

**EFFECT OF ANNEALING TEMPERATURE AND INDIUM DOPING ON
STRUCTURAL, OPTICAL AND ELECTRICAL PROPERTIES OF TIN OXIDE (SnO₂)
THIN FILMS DEPOSITED BY ULTRASONIC SPRAY TECHNIQUE**

K. Bennaceur¹, A. Attaf^{1,*}, H. Saidi¹, M.S. Aida², A. Bouhdjer¹, H. Ezzaouia³

¹ Physics of Thin Films and Applications Laboratory, University of Biskra, BP 145 RP, Biskra
07000, Algeria

² Laboratoire de Couches Minces et Interfaces Faculté des Sciences Université de Constantine,
Algeria

³ Laboratoire des semi-conducteurs, nanostructures et Technologie Avancée, Research and
Technology Centre of Energy, Borj-Cedria Science and Technology Park, BP 95, 2050
Hammam-Lif, Tunisia

Received: 28 February 2018 / Accepted: 26 April 2018 / Published online: 01 May 2018

ABSTRACT

Highly transparent and semiconducting indium-doped tin oxide films were deposited on a glass substrate at 400°C using an ultrasonic spray technique. The effect of In-content and annealing temperature on the structural, optical and electrical properties were examined. The X rays diffraction (XRD) analysis shows that In doped SnO₂ films have polycrystalline nature. The preferential orientations are sensitive to indium doping and annealing temperature. The films crystallite size and crystallinity are enhanced after annealing at 600°C for 30 min. The as-deposited films show low transmittance and low optical band gap that decrease with increasing In-content. The annealed films show minimum sheet resistance and their transmittance outrun 85 % in the visible region. These results are significant for the use of tin oxide in optoelectronic devices.

Keywords: In-doped SnO₂; High transparency; crystallinity; band gap.

Author Correspondence, e-mail: ab_attaf@univ-biskra.dz

doi: <http://dx.doi.org/10.4314/jfas.v10i2.7>



1. INTRODUCTION

For the past few decades, tin oxide (SnO_2) based transparent conducting oxide (TCO) thin films are gaining considerable attention in the new area of applications like optical and optoelectronic domains. SnO_2 exhibit better electrical conductivity with free carrier density in the order of 10^{18}cm^{-3} , thermal stability, optical transparency in the visible region. SnO_2 is a direct wide band gap semiconductor of $E_g \sim 3.6 \text{ eV}$ at room temperature [1]. Because of its unique optical and electrical properties, tin oxide thin films have been used in variety of applications such as transparent electrodes for solar cells [2], gas sensors [3,4], diodes [5], photocatalysis for waste water depollution[6] and anode in lithium batteries [7].

SnO_2 thin films exhibits n-type conductivity due to the presence of native defects i.e., non-stoichiometry (interstitial of tin (Sn_i) and oxygen vacancy (V_o)) [8]. It can be easily doped with a wide variety of ions to meet the demands of several application fields [9]. The elements used as dopants such as molybdenum (Mo), fluorine (F), lithium (Li), antimony (Sb), cobalt (Co), cerium (Ce) and Indium (In) [10-16].

Several deposition techniques have been used to prepare SnO_2 thin films, including: spray pyrolysis [17,18], chemical vapor deposition [19], reactive evaporation [20] dc and rf sputtering, sol-gel [21] and pulsed laser ablation [22]. Among these deposition methods, spray pyrolysis is a simple and inexpensive technique for large area coating [8].

In this study, indium-doped tin oxide (TO:In) films have been deposited by spray pyrolysis technique and the effect of doping and thermal annealing in the structural, electrical and optical properties are discussed.

2. EXPERIMENTAL PROCEDURE

Thin films of indium-doped SnO_2 (TO:In) with different concentrations (1 wt%, 2 wt%, 4 wt% and 8 wt %) were deposited using ultrasonic spray technique on glass substrates. Tin chloride penta-hydrate $\text{SnCl}_4 \cdot 5\text{H}_2\text{O}$ (99.0%) was used as tin source. Methanol CH_3OH was used as solvent and indium chloride InCl_3 (99.0%) was used as Indium dopant source. 0.1 mol/l of Tin chloride penta-hydrate was dissolved in an appropriate amount of methanol. Specific amounts of indium chloride were added into the previous solution. The solution was sprayed onto

heated glass substrates (400 °C) which was at a distance of 5 cm from the spray nozzle in atmospheric pressure for 5 min as a growth time. The solution flow rate was 50 mL/h. The films were annealed for 30 min at 600 °C in air.

Structural characterizations were analyzed by X-ray diffraction (XRD) on a D8 ADVANCE diffractometer with Cu K α radiation ($\lambda=1.5405$ Å). Optical transmission spectra were obtained using an UV–VIS–NIR spectrophotometer (UVI-3101 PC SHIMADZU). Electrical resistivity was measured by four probes method in dark ant at room temperature conditions. of second subtitle [3].

3. RESULTS AND DISCUSSION

3.1. X-ray diffraction studies

The XRD patterns for the as-deposited SnO₂.In thin films are shown in Fig.1.a. In the present study, all the prominent peaks in the pattern correspond to the rutile structure of SnO₂ and are indexed on the basis of JCPDS file no. 41-1445. As shown in Fig. 1.a, the intensity of (200) peak decreases with doping level, up to 4 wt.% In concentration, then increases. For the heavily Indium doped SnO₂ thin films (4 and 8 wt.%) the preferential orientation is changed to (101). The presence of other orientations such as (110), (211), (310) and (301) have also been detected. No indium oxide phases are found from the XRD patterns, which implies that In substitutes Sn in the tetragonal lattice or In probably segregates to the non-crystalline region in the grain boundaries. Similar behaviors was also observed by Caglar et al and Manoj et al using also indium as dopant [9,16].

Fig. 1.b. shows the diffraction patterns of SnO₂: In thin films annealed at 600°C. The XRD results indicate that all films are tetragonal rutile structure with a preferential orientation in the plane (200). Film annealed at 600°C exhibits intense XRD peaks, indicating film crystallinity improvement by comparison to the as-deposited films. This indicates that annealing at 600°C for 30 min is sufficient to organize the crystalline structure of the products and confirms the enhancement of the crystal quality of SnO₂ films [23].

In order to estimate the preferred orientation of the TO:In films, we use the texture coefficient (TC) which represents the texture of the particular plane, deviation of which from unity means

the preferred growth direction. The TC are calculated from Eq. (1) [24], for the reflections (1 1 0), (1 0 1), (2 0 0), (2 1 1), (310) and (3 0 1) are shown in Figs. 2.a and 2.b before and after annealing, respectively.

$$TC(hkl) = \frac{I(hkl) / I_0(hkl)}{N^{-1} \sum_n I(hkl) / I_0(hkl)} \quad (1)$$

Where $I(hkl)$ is the measured relative intensity of a plane (hkl) , $I_0(hkl)$ is the standard intensity of the plane (hkl) , N is the reflection number and n is the number of diffraction peaks.

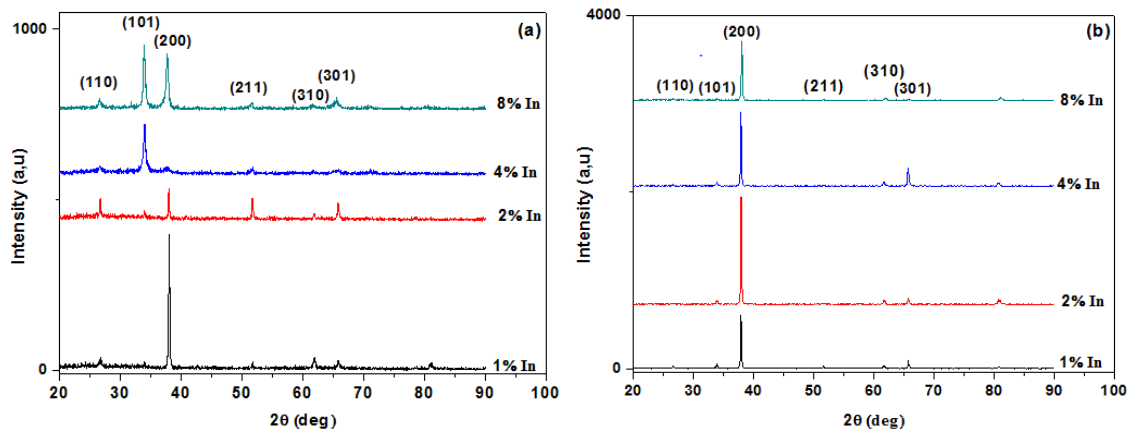


Fig.1. X-ray diffractograms of indium-doped tin oxide films with different indium concentration: (a) before annealing, (b) after annealing.

From the TC in Fig. 2.a it appears that at 1 wt.% and 2 wt.% the preferential (200) orientation is enhanced while the (101) orientation repressed. However, at 4 wt.% and 8 wt.% the preferential (200) orientation is suppressed while the (101) orientation is enhanced. Variation of the TCs with Indium content after annealing as shown in Fig.2.b All films have (200) preferred orientation and the highest TC value for each film belongs to (200).

Films crystallite size (G) was calculated for preferential orientations. Scherrer's equation [25] was used to estimate the crystallite size of In-doped SnO_2 films using its (101), (200) and (200) reflections before and after annealing, respectively (Fig. 3a and 3b).

$$G = \frac{K\lambda}{\beta \cos \theta} \tag{2}$$

Where k is a constant (0.94), β is the full width at half maximum (FWHM) value, λ is the wavelength of the CuK_α radiation source ($\lambda = 1.5418 \text{ \AA}$) and θ is the Bragg angle of the diffraction peaks.

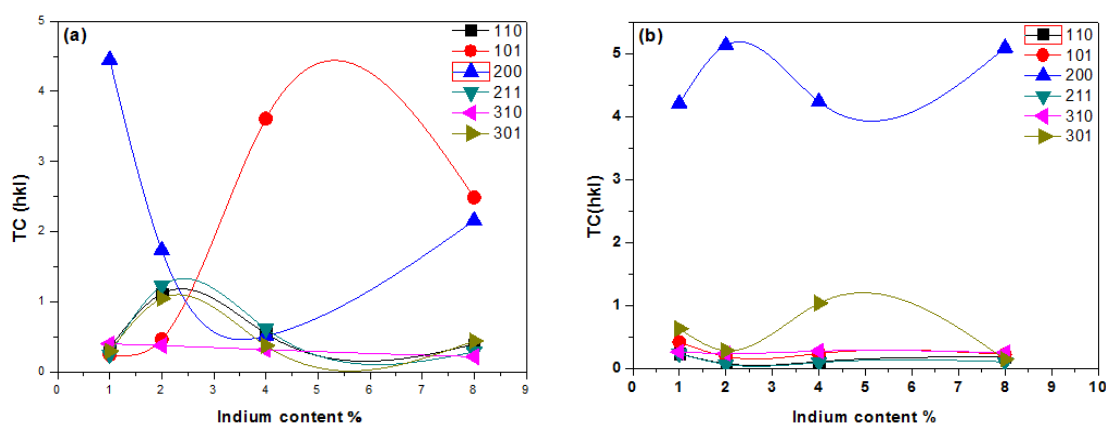


Fig.2. The variation of TC values with deposition Indium content: (a) before annealing (b) after annealing of (110), (101), (200) and (211) planes.

Table 1. Recapitulating measured values before and after annealing temperature at 600°C.

	Concentration of indium	G(nm)		Average G (nm)	δ (10^{15} lines/m ²)	E_g (eV)	E_u (eV)	R_s (k Ω /sq)
		(101)	(200)					
Before annealing	1	43,362	40,61	41,986	0.567	3,852	0,2917	50.21
	2	34,68	43,637	39,16	0.652	3,775	0,3118	140.12
	4	18,978	7,49	13,234	5.710	3,756	0,3293	500.2
	8	23,82	19,564	21,692	2.130	3,549	0,3562	950
After annealing	1	-	46,895	46,895	0.455	4,3816	0,268	21.1
	2	-	46,15	46,15	0.469	3,898	0,279	40.4
	4	-	44,51	44,51	0.505	3,725	0,326	201.3
	8	-	39,879	39,879	0.629	3,665	0,344	345.6

The results calculated are listed in Table 1. We found that the crystallite size decreased with indium concentration increase (before and after annealing). This may probably due to the

effect of recrystallization process because of doping [16]. It is also observed that the full width at half maxima (FWHM) increases with an increase in indium content in the SnO₂ thin films. This suggests that indium incorporation in the SnO₂ lattice results in a decrease in crystallite size [26].

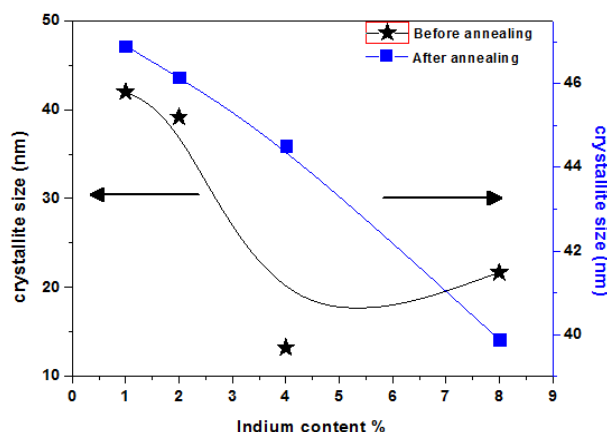


Fig.3. The variation of the crystallite size with deposition In content of SnO₂ films before and after annealing temperature at 600°C.

As can be seen, the crystallite sizes were varied in the range of 7.49-43.637 nm for the as deposited films, while it became in the range 39.879-46.895 nm after annealing (see Table 1). The crystallite sizes of the as deposited films are smaller than the annealed ones. The increase in the nanocrystals size and the crystallinity improvement after annealing temperature can be attributed to enhancement of atoms kinetic energy at high temperature that assists more atoms move to more stable states in the lattice points [27]. Similar results were reported for F-doped [28] Ga-doped [29] and Mn-doped [30] SnO₂ thin films.

Using grain size values, the dislocation density (δ), defined as the length of dislocation lines per unit volume of the crystal was calculated by using the Williamson and Smallman's formula [31]:

$$\delta = \frac{1}{G^2} \quad (3)$$

The dislocation density values (see table.1) of the films are increasing with increasing the In content and change inversely with G of the films.

3.2. Optical and electrical studies

Fig. 4 shows the transmittance spectra of Indium doped SnO₂ thin films for both as-deposited and annealed, where for longer wavelengths ($\lambda > 400$ nm) all films become transparent. Where the film exhibits significant oscillations in long wavelength; this oscillation may be due to the roughness of SnO₂ film top surface which can generate interference phenomenon, even at nuded eye one can see that the SnO₂ film is very smooth [17].

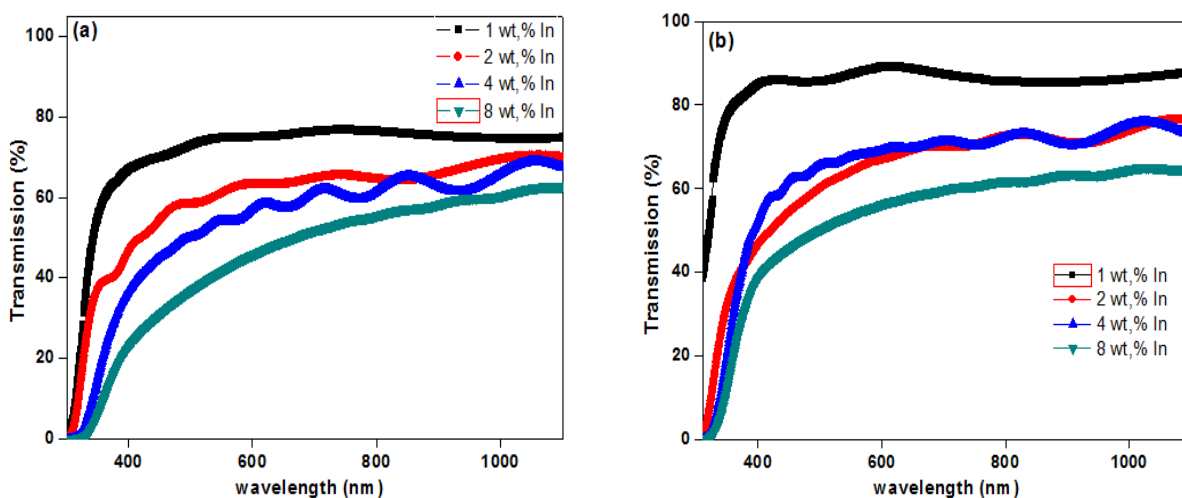


Fig.4. Optical transmittance T(%) versus wavelength λ of TO:In films at various indium amounts (a) before annealing,(b) after annealing

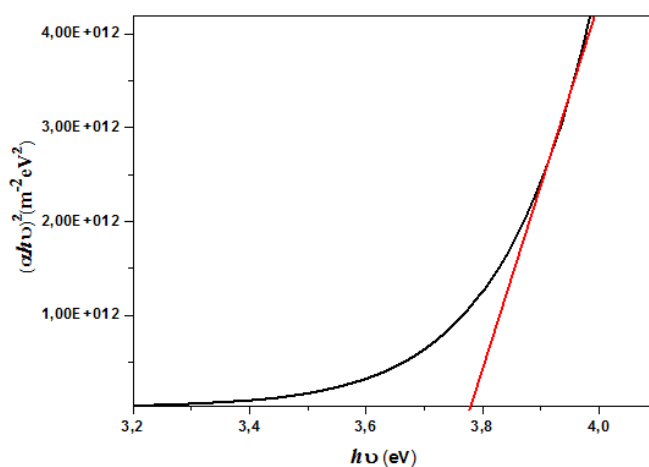


Fig.5. The plot of $(\alpha h\nu)^2$ vs. $(h\nu)$ for SnO₂:In film

Table 2. Transmittance values of In-doped SnO₂ thin films before and after annealing temperature

	Concentration of indium	Transmittance (%)						
		450nm	550nm	650nm	750nm	850nm	950nm	1050nm
Before Annealing	1	70.14	75.14	75.758	77.022	76.067	75.14	74.831
	2	54.466	61.348	63.539	65.73	65.112	67.612	70.449
	4	45.084	54.157	57.303	60.421	64.494	61.994	68.876
	8	30.983	41.629	48.848	53.848	56.966	59.803	62.303
After Annealing	1	86.095	87.668	88.904	86.713	85.786	86.095	87.359
	2	54.775	64.185	69.494	70.758	72.64	71.376	76.376
	4	61.994	67.612	69.494	70.14	72.64	71.994	75.449
	8	45.702	53.539	58.23	60.73	62.303	63.23	64.803

The transmittance values of films at 450 nm, 550 nm, 650 nm, 750 nm, 850 nm, 950 nm and 1050 nm are shown in Table 2. at 550 nm, the highest value of transmittance is reached 75.14% for 1% TO:In (before annealing) and 87.668% for 1% TO:In (after annealing). It is observed that the transmittance is lower for as-deposited films than that of annealed films over the wavelength region ~400 nm to 1100 nm.

From Table 2, it can be seen that optical transmittance reduces with increasing In doping. This is attributed to the reduction in the crystallite sizes after In atoms incorporation. The absorption edges for the annealed films shift to shorter wavelength compared with that of as-deposited films, which is due to Burstein–Moss effect [32,33] as shown in Fig. 4. The fundamental absorption edge can be used to calculate films optical band gap, E_g . It was estimated by plotting $(\alpha h\nu)^2$ against the photon energy ($h\nu$) and is shown in Fig. 5. The linear nature of the plot indicates the existence of direct transition.

The extrapolation of straight line to $h\nu=0$ axis gives the value of the band gap (see Fig. 5) according to the following equation [34]:

$$(\alpha h\nu) = A(h\nu - E_g)^{1/2} \quad (4)$$

Where A is a constant, $h\nu$ the photon energy and E_g is the optical band gap. On the other hand, we have used the Urbach energy (E_u), which is related to the disorder in the film network, as it is expressed below [35]:

$$A = A_0 \exp\left(\frac{h\nu}{E_u}\right) \quad (5)$$

Where A_0 is a constant, $h\nu$ is the photon energy and E_u is the Urbach energy.

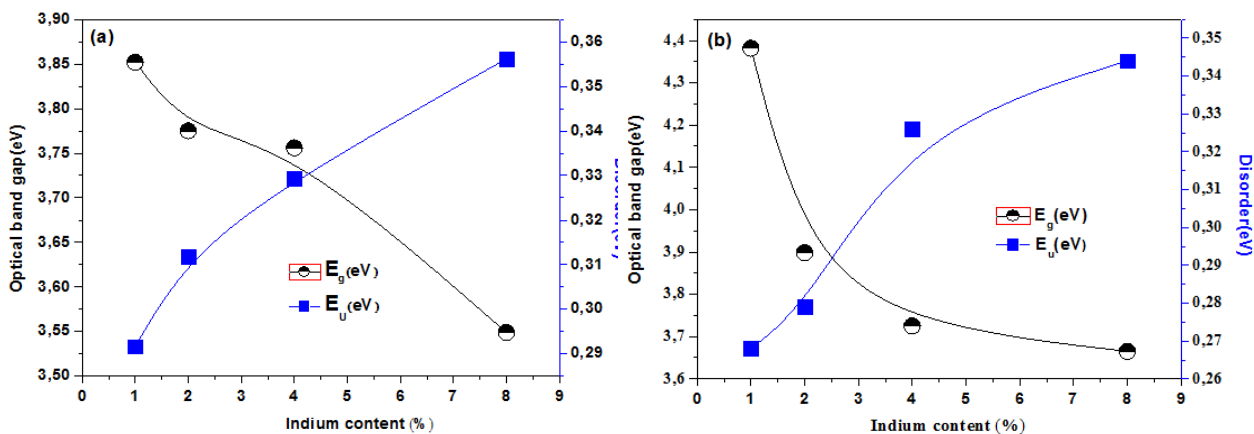


Fig.6. The variation of optical band gap and disorder of TO:In films at various indium amounts (a) before annealing, (b) after annealing

The values of the optical band gap energy before and after annealing were listed in Table 1. The Urbach energy E_u is also given on the same table. The value of E_g is in the range of 3,85-3,54 eV, which is in good agreement with the previously reported values [36,37], and 4,38-3,66 eV for both as-deposited and annealed films, respectively. As clearly seen in Figs. 6.a and 6.b, the band gap energy, E_g , decreases with increasing In content. The narrowing band gap energy is possibly due to the existence of In impurities in the SnO_2 structure, which induces new recombination centers formation with lower emission energy [9]. Moreover, the dislocation density increase with increasing In doping ratio (see table 1), this increase of δ gives rise to disorders and crystal defects in the SnO_2 lattice. This may cause to a decrease of the E_g values with In doping. Many authors have reported the red shift of E_g by different dopant in the SnO_2 [38-40]. However, the band gap energy is lower for as-deposited films than that of annealed films (see Figs. 6.a and 6.b). This is due to the reduction of disorder in the film due to the improvement in crystalline quality of this layer [41], and the band tail width values, E_u , of these films confirm this hypothesis (see table 1). El Sayed et al. [1] also reported the narrowing of E_g of SnO_2 :Co.

The effect of In content and annealing on the sheet resistance of SnO₂:In films was studied. Films sheet resistances R_s , are tabulated in Table 1. From this table, it is noted that R_s value increases with increasing In concentration for both as-deposited and annealed films. Before annealing, the grain boundaries arise due to the development of small size grains due to In incorporation, and the incomplete bondings between atoms act as charge carriers traps and thus increases the sheet resistance [42]. Large additions of Sb, P, Tl and In increased the resistance and reduced the charge carrier concentration. According to them these effects are probably associated with the observed increased disorder and altered crystallographic orientation in the films [16]. In the present work, the preferred orientation changes from (200) to (101) when the doping increases. Comparable behavior has been reported in the literature[43]. Dobler et al. [44] explained that doping with elements having less than 4 valency (such In) leads to electron density decreasing, causing thereafter, the material resistivity enhancement. The R_s values for annealed films are lower than R_s of those as-deposited films. This reduction is attributed to films oxygen deficiency. It is well know that film oxygen deficiency yields to films blackening [45]. Furthermore, annealing enhances the crystal structure and grain boundaries reduction, this leads to the decrease in films resistivity [46].

4. CONCLUSIONS

In-doped SnO₂ films were deposited by ultrasonic spray technique onto glass substrates. Effect of annealing and In content on SnO₂ films structural, optical and electrical properties were investigated. As evidenced from X-ray diffraction analysis, films crystallite size increases with annealing, while it is reduced with increasing In content. The crystal quality is improved by annealing, in contrary to In doping that do not yield to an improvement in crystal quality. The optical measurements indicated that films transmittance improves with annealing but decreases with indium concentrations. Moreover the optical band gap is narrowed with increasing In content and shifts to shorter wavelength with annealing. The films sheet resistance was found to increase with In content but decrease with annealing temperature. We inferred that In doping and annealing may be used as band gap and particle size tailoring

process for an efficient use of SnO₂ films in optoelectronic devices.

5. REFERENCES

- [1] A.M. El Sayeda, S. Taha, Mohamed Shaban, G. Said, Superlattices and Microstructures, 95 (2016) 1-13.
- [2] Chitra Agashe, J. Hüpkens, G. Schöpe, M. Berginski, Sol. Energy Mater. Sol. Cells, 93 (2009) 1256–1262.
- [3] L.A. Patil, M.D. Shinde, A.R. Bari, V.V. Deo, Sens. Actuators B 143 (2009) 270–277.
- [4] J. Kaur, R. Kumar, M.C. Bhatnagar, Sens. Actuators B 126 (2007) 478–484.
- [5] T. Yang, X. Qin, H. Wang, Qu. Jia, Runsheng Yu, B. Wang, J. Wang, K. Ibrahim, X. Jiang, Qu. He, Thin Solid Films 518 (2010) 5542–5545.
- [6] A. Enesca, M. Baneto, D. Perniua, L. Isac, C. Bogatua, A. Duta, Applied Catalysis B: Environmental 186 (2016) 69–76.
- [7] V. Subramanian, K.I. Gnanasekar, B. Rambabu, Solid State Ionic 175 (2004) 181–184.
- [8] P. Ravikumar, K. Ravichandran, B. Sakthivel, J. Mater. Sci. Technol., 2012, 28(11), 999–1003
- [9] M. Caglar, K. Cemil Atar, Spectrochimica Acta Part A: Molecular and Biomolecular Spectroscopy, 96 (2012) 882–888
- [10] D.D. Purkayastha, M.G. Krishna, V. Madhurim, Mater. Lett. (2014) 21-23.
- [11] J.T. Wang, X.L. Shi, X.H. Zhong, J.N. Wang, L. Pyrah, K.D. Sanderson, P.M. Ramsey, M. Hirata, K. Tsuru, Sol. Energy Mater. Sol. C 132 (2015) 578-588.
- [12] D. Paul Joseph, P. Renugambal, M. Saravanan, S. Philip Raja, C. Venkateswaran, Thin Solid Films 517 (2009) 6129–6136.
- [13] Ch.M. Wang, Ch.C. Huang, J.Ch. Kuo, J.L. Huang, Surf. Coat. Technol. 231 (2013) 374–379.
- [14] G. Korotcenkov, I. Boris, V. Brinzari, S.H. Han, B. K. Cho, Sens Actuat B 182 (2013) 112–124.
- [15] Z. Jiang, Z. Guo, B. Sun, Y. Jia, M. Li, J. Liu, Sens Actuat B 145 (2010) 667–673.
- [16] P.K. Manoj, Benny Joseph, V.K. Vaidyan, D. Sumangala Devi Amma, Ceram.Int. 33(2007) 273–278.

-
- [17] H. Bendjedidi, A. Attaf, H. Saidi, M. S. Aida, S. Semmari, A. Bouhdjar, and Y. Benkhetta, *Journal of Semiconductors*. Vol. 36, No. 12
- [18] C. Khelifi, A. Attaf, H. Saidi, Anouar Yahia, Mohamed Dahnoun, Abdelhakim Saadi, *Optik* 127 (2016) 11055–11062.
- [19] J.J. Berry, D.S. Ginley, P.E. Burrows, *Appl. Phys. Lett.* 92 (2008) 193304.
- [20] K. Omura, P. Veluchamy, M. Tsuji, T. Nishio, M. Murozono, *J. Electrochem. Soc.* 146 (1999) 2113.
- [20] B.D. Ann, S.H. Oh, D.U. Hong, D.H. Shin, A. Moujoud, H.J. Kim, *Cryst. Growth* 310 (2008) 3303.
- [21] M.-M. Bagheri-Mohagheghi, M. Shokooh-Saremi, *J. Phys. D Appl. Phys.* 37 (2004) 1248.
- [22] A.N. Banerjee, R. Maity, P.K. Ghosh, K.K. Chattopadhyay, *Thin Solid Films* 474 (2005) 261.
- [23] J. Henry, K. Mohanraj, G. Sivakumar, S. Umamaheswari, *Spectrochim. Acta A* 143 (2015) 172-178.
- [24] F. Bouaichi, H. Saidi, A. Attaf, M. Othmane, N. Lehraki, M. Nouadji, M. Poulain and Said Benramache, *Main Group Chemistry* 15 (2016) 57–66.
- [25] S. Rani, P. Suri, P.K. Shishodia, R.M. Mehra, *Sol. Energy Mater. Sol. Cells* 92 (2008) 1639–1645.
- [26] J. Kaur, R. Kumar, M.C. Bhatnagar, *Sensors and Actuators B* 126 (2007) 478–484.
- [27] R. Lotfi Orimi, M. Maghouli, *Optik* 127 (2016) 263–266.
- [28] Sh. J. Ikhmayies, *international journal of hydrogen energy* xxx (2016) 1-8.
- [29] C.-Y. Tsay, S.C. Liang, *J. Alloy. Compd.* 622 (2015) 644-650.
- [30] F. Ghodsi, J. Mazloom, *Appl. Phys. A Mater.* 108 (2012) 693-700.
- [31] G.K. Williamson, R.E. Smallman III, *Philos. Mag.* 1 (1956) 34–45.
- [32] E. Burstein, *Phys. Rev.* 93 (1954) 632–633.
- [33] T.S. Moss, *Section B* 57 (1954) 775.
- [34] A. Bouhdjer, A. Attaf, H. Saidi, H. Bendjedidi, Y. Benkhetta, and I. Bouhaf, *Journal of Semiconductors*. Vol. 36, No. 8.

- [35] Mohamed Othmane, Abdallah Attaf, Hanane Saidi, Fouad Bouaichi, Nadia Lehraki, Malika Nouadji, Marcel Poulain, International Journal of Nanoscience. Vol. 15, Nos. 1 & 2 (2016) 1650007.
- [36] E. Çetinörgü, Optics Communications 280 (2007) 114–119.
- [37] M.-M. Bagheri-Mohagheghi, N. Shahtahmasebi, M.R. Alinejad, A. Youssefi, M.Shokooh-Saremi, Solid State Sciences 11 (2009) 233–239.
- [38] S. Vijayalakshmi, S. Venkataraj, M. Subramanian, R. Jayavel, Journal of Physics D: Applied Physics 41 (2008) 035505
- [39] S.S. Pan, Y.X. Zhang, X.M. Teng, G.H. Li, L. Li, Journal of Applied Physiology 103(2008) 093103.
- [40] L.M. Fang, X.T. Zu, Z.J. Li, S. Zhu, C.M. Liu, L.M. Wang, F. Gao, Journal of Material Science Materials in Electronics 19 (2008) 868–874.
- [41] N. Lehraki, M.S. Aida, S. Abed, N. Attaf, A. Attaf, M. Poulain, Current Applied Physics 12 (2012) 1283-1287.
- [42] K.-Mu Lee, K.-Liang Shih, C.-Hung Chiang, V. Suryanarayanan, C.-Guey Wu, Thin Solid Films 570 (2014) 7-15.
- [43] Mark E. White, Oliver Bierwagen, Min Ying Tsai, James S. Speck, Appl. Phys. Expr. 3 (2010) 051101–51103.
- [44] D. Dobler, S. Oswald, G. Behr, J. Werner, K. Wetzig, Cryst. Res. Technol. 38 (2003) 956–961.
- [45] W.F. Wu and B.S. Chiou, Thin Solid Films, 247(1994) 201.
- [46] W. Mao, B. Xiong, Q. Li, Y. Zhou, C. Yin, Y. Liu, C. He, Phys. Lett. A 379 (2015) 1946-1950.

How to cite this article:

Bennaceur K, Attaf A, Saidi H, Aida MS, Bouhdjer A, Ezzaouia H. Effect of annealing temperature and Indium doping on structural, optical and electrical properties of tin oxide (SnO₂) thin films deposited by ultrasonic spray technique. J. Fundam. Appl. Sci., 2018, 10(2), 84-96.